Rapid Communications

Pressure-induced magnetism in the iron-based superconductors $A\mathrm{Fe_2As_2}$ (A = K, Cs, Rb)

Rustem Khasanov,[1,*] Zurab Guguchia,[1] Elvezio Morenzoni,[1] Chris Baines,[1] Aifeng Wang,[2] Xianhui Chen,[2] Zbigniew Bukowski,[3] and Fazel Tafti[4,5]

[1]*Laboratory for Muon Spin Spectroscopy, Paul Scherrer Institute, CH-5232 Villigen PSI, Switzerland*

[2]*Hefei National Laboratory for Physical Sciences at Microscale and Department of Physics, University of Science and Technology of China, Hefei, Anhui 230026, China*

[3]*Institute of Low Temperature and Structure Research, Polish Academy of Sciences, PL-50-422 Wroclaw, Poland*

[4]*Department of Physics, Boston College, Chestnut Hill, Massachusetts 02467, USA*

[5]*Département de physique & RQMP, Université de Sherbrooke, Sherbrooke, Québec, Canada J1K 2R1*

(Received 6 May 2020; accepted 18 September 2020; published 2 October 2020)

The magnetic properties of iron-based superconductors $A\mathrm{Fe_2As_2}$ (A = K, Cs, and Rb), which are characterized by the V-shaped dependence of the critical temperature (T_c) on pressure (P), were studied by means of the muon spin rotation/relaxation technique. In all three systems studied the magnetism was found to appear for pressures slightly below the critical one (P_c), i.e., at pressure where $T_c(P)$ changes the slope. Rather than competing, magnetism and superconductivity in $A\mathrm{Fe_2As_2}$ are coexisting at the $P \gtrsim P_c$ pressure region. Our results support the scenario of a transition from one pairing state to another, with different symmetries on either side of P_c.

DOI: 10.1103/PhysRevB.102.140502

Since the discovery of iron-based superconductors, much effort has been devoted to identify the pairing mechanism responsible for their high critical temperature [1,2]. While some properties of iron-based superconductors are reminiscent of the cuprate superconductors, the differences between the two families are considerable. Iron-based superconductors (Fe-SCs) are generally believed to have s-wave pairing symmetry. They are multiband superconductors, with an energy gap that varies significantly among the various Fermi-surface sheets [3]. Their gap structure is not universal and is subject to change as a function of doping, external, or chemical pressure [4]. Recent theoretical works using a five-orbital tight-binding model show a near degeneracy between d and $s^{\pm}$ pairing states in Fe-SCs as a result of the multiorbital structure of the Cooper pairs and the near nesting conditions [5,6].

Hydrostatic pressure is a clean tuning parameter that can modify the orbital overlap, the exchange interactions, and the band structure of metals. Given the near degeneracy between different pairing states, it is conceivable that the pairing symmetry of certain Fe-SCs might be tuned by pressure [7–13]. Such an idea leads, in particular, to the observation of a V-shaped T-P phase diagram in $A\mathrm{Fe_2As_2}$ (A = K, Cs, and Rb), where the transition temperature T_c decreases initially as a function of pressure, then at a critical pressure P_c, it suddenly changes direction and increases [7–9] or remains almost constant at least up to pressures ∼4 GPa [10,13–15]. The constancy of the Hall coefficient through P_c rules out a change in the Fermi surface [7,8,11]. In the case of $\mathrm{KFe_2As_2}$ this was additionally confirmed by de Haas–van Alphen measurements, showing quantum oscillations that smoothly evolve across P_c [9]. In the absence of any sudden change in the Fermi surface across the critical pressure P_c, the resistivity and magnetic susceptibility experiments of Refs. [7,8,10,11] detect a sudden change of the upper critical field $H_{c2}(T)$, which is interpreted as evidence of a sudden change in the structure of the superconducting energy gap across P_c.

In this Rapid Communication, we report on zero-field (ZF) and longitudinal-field (LF, where a magnetic field is applied parallel to the initial muon-spin polarization) muon-spin rotation (μSR) studies of $A\mathrm{Fe_2As_2}$ (A = K, Cs, and Rb) as a function of pressure. In all three systems studied the magnetism was found to appear for pressures slightly below the critical one (P_c), i.e., at pressure where $T_c(P)$ changes the slope. Rather than compete [16], magnetism and superconductivity in $A\mathrm{Fe_2As_2}$ are coexisting at the $P \gtrsim P_c$ pressure region. Our findings reveal an intriguing interplay of magnetism and superconductivity in $A\mathrm{Fe_2As_2}$, whereby the former supports (or even enhances) the latter, in contrast to the usual suppression caused by phase competition.

Polycrystalline samples of $\mathrm{KFe_2As_2}$, $\mathrm{CsFe_2As_2}$, and $\mathrm{RbFe_2As_2}$ were synthesized by the conventional solid state reaction method using AAs (A = K, Cs, and Rb) and $\mathrm{Fe_2As}$ as starting materials [17,18]. AAs was prepared by reacting stoichiometric alkali-metal pieces and As powders at 200 °C for 4 h in an evacuated quartz tube, and $\mathrm{Fe_2As}$ was synthesized by heating Fe and As powders at 700 °C for 24 h. Stoichiometric amounts of the starting materials were first thoroughly grounded, pressed into pellets, and finally sealed in a Nb tube under 1.5 atm of argon gas. The Nb tube was then sealed in an evacuated quartz tube and heated to 650 °C for 36 h. All the sample preparation processes were carried out in a glove box under high-purity argon atmosphere. The powder x-ray diffraction patterns are consistent with those reported in

*Corresponding author: rustem.khasanov@psi.ch

Ref. [19]. Detailed information on the sample characterization is given in the Supplemental Material [20].

The pressure was generated in double-wall piston-cylinder types of cells especially designed to perform muon-spin rotation/relaxation (μSR) experiments under pressure [21,22]. As a pressure transmitting medium 7373 Daphne oil was used. The maximum safely reachable pressure is $\sim$2.7 GPa. The pressure was measured *in situ* by monitoring the pressure-induced shift of the superconducting transition temperature of In [22].

Zero-field and longitudinal-field μSR measurements were performed at the πM3 and μE1 beam lines (Paul Scherrer Institute,Villigen, Switzerland), by using the dedicated LTF and GPD spectrometers, respectively. At the LTF spectrometer, equipped with a dilution fridge cryostat, ZF-μSR experiments at ambient pressure and down to temperatures $\simeq$20 mK were carried out. At the GPD spectrometer [21], equipped with an Oxford sorption pumped ^{3}He cryostat (base temperature $\sim$0.24 K), ZF and LF-μSR experiments under a pressure up to $\sim$2.7 GPa were conducted. The typical counting statistics were ~ 5–7×10^6 decay positron events for each particular data point. The data were analyzed using the free software package MUSRFIT [23].

The magnetic response of AFe$_2$As$_2$ at ambient pressure was studied in a set of ZF-μSR measurements at the LTF instrument. A few representative μSR time spectra taken below and above the superconducting transition temperature for KFe$_2$As$_2$, CsFe$_2$As$_2$, and RbFe$_2$As$_2$ are shown in the Supplemental Material [20] and in Ref. [18]. No sign of magnetism was detected in the ZF-μSR response of RbFe$_2$As$_2$ [18]. The experimental data are well described by a standard Kubo-Toyabe depolarization function [24], reflecting the field distribution at the muon site created by the nuclear moments. In KFe$_2$As$_2$ and CsFe$_2$As$_2$, an exponential relaxation was found to be present in the ZF-μSR signal at ambient pressure and it increases slightly with decreasing temperature, thus pointing to the presence of magnetism. The absence of spontaneous oscillations indicates that there is no onset of long-range magnetic order. It was also found that the relaxation occurs only in part of the sample volume ($\simeq$70% in a case of KFe$_2$As$_2$ and $\simeq$40% in a case of CsFe$_2$As$_2$), while the rest of the sample displays a nonrelaxing behavior, typical of a nonmagnetic fraction (see the Supplemental Material [20]).

We think that the magnetic signal observed at the ambient pressure in KFe$_2$As$_2$ and CsFe$_2$As$_2$ is not intrinsic for these compounds but caused by the presence of a small amount of magnetic impurities in the samples studied. Our conclusions are based on the following arguments:

First, our longitudinal field (LF) μSR experiments of KFe$_2$As$_2$ show that at $T = 0.25$ K, the slow-relaxing component associated with the ambient pressure impurity magnetism [$\lambda_{\rm Imp}(0.25\ {\rm K}) \simeq 0.55\ \mu{\rm s}^{-1}$] recovers at fields of the order of 2 mT (see Supplemental Material [20]). Such behavior is expected in a case of diluted and randomly oriented magnetic moments giving rise to weak magnetism [24,25].

Second, the weak ambient pressure magnetism does not occupy the whole sample volume. A substantial part of the KFe$_2$As$_2$ and CsFe$_2$As$_2$ samples remains nonmagnetic down to the lowest temperature [20].

Third, ZF-μSR studies of the superconducting Ba$_{1-x}$K$_x$F$_2$As$_2$ with $0.5 \leqslant x \leqslant 0.9$ [26] show the absence of any kind of magnetic response. The ZF-μSR time spectra were well described by a single-component exponential relaxation function with a weak depolarization rate $\lambda \simeq 0.01$–$0.04\ \mu{\rm s}^{-1}$. Note that these values are slightly smaller but comparable to $\lambda(T) \simeq 0.08\ \mu{\rm s}^{-1}$ for $T \gtrsim 1$ K as obtained in our study [20].

Fourth, μSR experiments on a high-quality KFe$_2$As$_2$ single-crystal performed by Ohishi [27] also show a temperature-independent ZF-μSR time spectra down to $T \simeq 20$ mK with $\lambda \simeq 0.05\ \mu{\rm s}^{-1}$.

Fifth, no ambient pressure magnetism was detected for the RbFe$_2$As$_2$ sample [18] and for the second (the "cross-checked") KFe$_2$As$_2$ sample.

As a next step, ZF-μSR experiments under a pressure were performed at the GPD instrument. Figure 1 shows ZF-μSR time spectra taken at various pressures and temperatures for all three systems studied. The buildup of an additional relaxing component, reflecting the presence of the pressure-induced magnetism, is clearly visible in the spectra.

In the case of KFe$_2$As$_2$ [Figs. 1(a) and 1(b)] the fast relaxing component starts to develop for pressures exceeding $P \gtrsim 1.6$ GPa. The absence of discrete frequency oscillations indicates that the magnetism is highly disordered. The amplitude of this fast relaxing component saturates above 1.78 GPa at $T = 0.27$ K and increases continuously with increasing pressure above $P \simeq 1.8$ GPa at $T \simeq 5$ K. Pressure-induced magnetism is also clearly visible in CsFe$_2$As$_2$ and RbFe$_2$As$_2$ in Figs. 1(c) and 1(e), respectively. In both systems at $T \simeq 0.25$ K an additional relaxing contribution starts to develop for pressures exceeding $\sim$0.7 GPa. These additional relaxations are less pronounced in RbFe$_2$As$_2$ compared to CsFe$_2$As$_2$ and in CsFe$_2$As$_2$ compared to KFe$_2$As$_2$.

The pressure-induced magnetism observed in AFe$_2$As$_2$ could arise either from static field distributions or fluctuating fields. In order to distinguish between these two possibilities, LF-μSR experiments on KFe$_2$As$_2$ were performed at $P = 1.8$ and 2.6 GPa (see the Supplemental Material [20]). At both pressures studied the full muon-spin polarization was found to recover at the longitudinal field $B_{\rm LF} \sim 0.2$–0.4 T, thus implying that the disordered pressure-induced magnetism in KFe$_2$As$_2$ is static [28].

We stress that the character of this disordered static magnetism appearing under pressure is very different from the impurity magnetism detected in KFe$_2$As$_2$ and CsFe$_2$As$_2$ at ambient pressure (see Figs. 7 and 8 in the Supplemental Material [20]).

First, the impurity magnetism, which is already present in the μSR spectra at the lowest pressure ($P \simeq 0.2$ GPa), is clearly different from that observed in spectra taken at $P \gtrsim 1.6$ GPa for KFe$_2$As$_2$ [Figs. 1(a) and 1(b)] and at $P \gtrsim 1.0$ GPa for CsFe$_2$As$_2$ [Fig. 1(c)].

Second, in the case of KFe$_2$As$_2$ the relaxation is much stronger at high pressures (see the inset in Fig. 2) and the magnetism itself extends up to much higher temperatures than that observed at ambient and low pressures.

Third, as will be shown later, in KFe$_2$As$_2$ for temperatures below $T \simeq 0.5$ K and pressures above $P \simeq 1.8$ GPa the

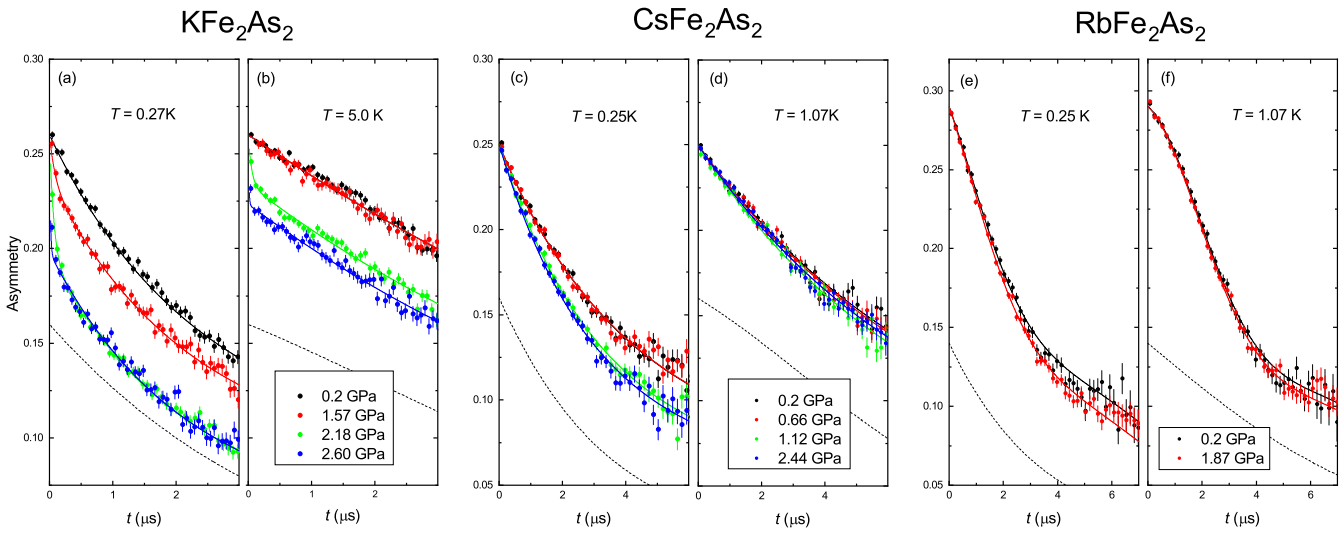

FIG. 1. Zero-field μSR time spectra measured at various pressures and temperatures: (a) and (b) in KFe_2As_2 at $P = 0.2$, 1.57, 2.18, and 2.60 GPa and at $T = 0.27$ and 5.0 K, respectively. (c) and (d) in $CsFe_2As_2$ at $P = 0.2$, 0.66, 1.12, and 2.44 GPa and at $T = 0.25$ and 1.07 K. (e) and (f) in $RbFe_2As_2$ at $P = 0.2$ and 1.87 GPa and at $T = 0.25$ and 1.07 K. The solid lines are fits of Eq. (1) with the sample part described by Eq. (2) for KFe_2As_2 and Eq. (3) for $CsFe_2As_2$ and $RbFe_2As_2$, respectively. The dashed lines are the background (pressure cell) contributions. See text for details.

high-pressure magnetism occupies almost 100% of the sample volume (see Figs. 2 and 3).

Finally, the similar pressure-induced magnetism was found in the second (the "cross-checked") KFe_2As_2 sample, which has no detectable amount of magnetic impurity fraction (see the Supplemental Material [20] for details).

The ZF high-pressure data were analyzed with the signal decomposed in contributions of the sample (s) and the pressure cell (pc),

$$A(t) = A_s(0)P_s(t) + A_{pc}(0)P_{pc}(t). \quad (1)$$

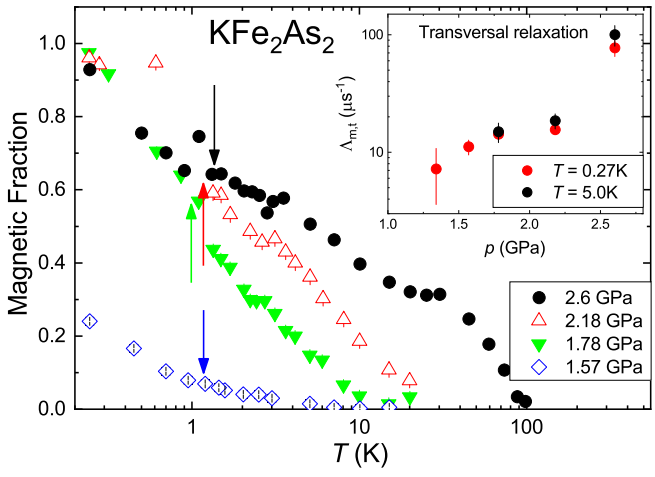

FIG. 2. Temperature dependence of the magnetic volume fraction f of KFe_2As_2 as obtained from the fit of Eq. (1) [with the sample contribution described by Eq. (2)] to the ZF-μSR data taken at $P = 1.57$, 1.78, 2.18, and 2.6 GPa. Arrows indicate the position of $T_c(P)$'s. The inset shows the pressure dependence of the fast relaxing component $\Lambda_{m,t}$.

Here, $A_s(0)$ and $A_{pc}(0)$ are the initial asymmetries and $P_s(t)$ and $P_{pc}(t)$ are temperature evolutions of the muon-spin polarization belonging to the sample and the pressure cell, respectively. Note that in pressure experiments a large fraction of the muons (roughly 50%) stops in the pressure cell walls, providing a background contribution [21]. The pressure cell contribution to the polarization signal $P_{pc}(t)$ was measured in an independent experiment.

In order to account for the strong magnetism in KFe_2As_2 the response of the sample was assumed to consist of "magnetic" and "nonmagnetic" (including an impurity contribution [Imp(t)] as described the Supplemental Material [20]) terms and is derived as

$$P_s(t) = \left[f\left(\tfrac{1}{3}e^{-\Lambda_{m,l}t} + \tfrac{2}{3}e^{-\Lambda_{m,t}t}\right) + (1-f)G_{KT}(t)\right] \times \mathrm{Imp}(t). \quad (2)$$

Here, f is the relative weight (volume) of the pressure-induced magnetic fraction. $\Lambda_{m,l}$ and $\Lambda_{m,t}$ are the exponential depolarization rates representing the longitudinal (1/3) and the transversal (2/3) relaxing components within the parts of the sample being in the magnetic state [24]. $G_{KT}(t) = 1/3 + 2/3(1-\sigma_s^2t^2)e^{-\sigma_s^2t^2/2}$ is the Gaussian Kubo-Toyabe depolarization function reflecting the field distribution created by the nuclear moments, and σ_s is the Gaussian depolarization rate caused by them [24]. During the fit the Imp(t) term was fixed to that obtained in the ZF experiments under the ambient pressure (see the Supplemental Material [20]). The solid lines in Figs. 1(a) and 1(d) represent the result of the fit of Eq. (1) to the ZF-μSR KFe_2As_2 data with the sample part described by Eq. (2).

Figure 2 shows the dependence of the magnetic volume fraction f of KFe_2As_2 on temperature for $P = 1.57$, 1.78, 2.18, and 2.6 GPa. The inset shows the pressure dependence of the fast relaxing component $\Lambda_{m,t}$. Note that for $P \lesssim$ 1.3 GPa the fit of Eq. (2) to the experimental data result in f

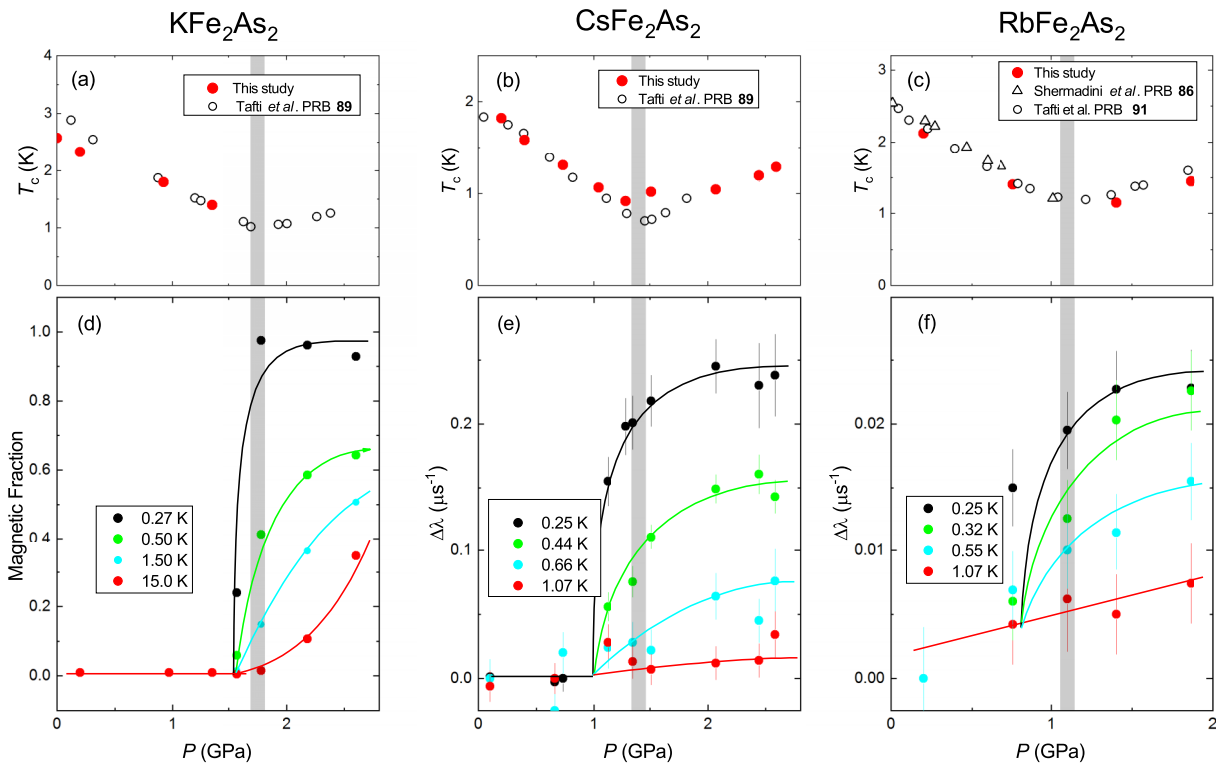

FIG. 3. (a) Dependence of the superconducting transition temperature T_c on P of KFe_2As_2. The red symbols are $T_c(P)$'s obtained in the present study in transverse-field μSR experiments [20]. The open symbols are $T_c(P)$ points from Ref. [8]. (b) and (c) The same as in (a) but for $CsFe_2As_2$ and $RbFe_2As_2$, respectively. The open symbols in (c) are $T_c(P)$ data from Refs. [11,57]. (d) Dependence of the magnetic volume fraction f of KFe_2As_2 on pressure at $T = 0.27$, 0.50, 1.50, and 15.0 K. (e) Dependence of the additional exponential relaxation $\Delta\lambda$ of $CsFe_2As_2$ on pressure for $T = 0.25$, 0.44, 0.66, and 1.07 K. (f) Same is in (e) but for $RbFe_2As_2$ and at $T = 0.25$, 0.32, 0.55, and 1.07 K. The gray stripes are the critical pressure regions where the transition temperature $T_c(P)$ changes the tendency from decreasing to increasing. The solid lines in (c)–(f) are guides for the eye.

being close to zero, thus implying that at low pressures the KFe_2As_2 sample is "nonmagnetic" with only the impurity magnetism as observed in the ZF-μSR experiment under ambient pressure. The data presented in Fig. 2 show that with increasing pressure an increasingly large part of the sample becomes magnetic. More important, for pressures exceeding $P \simeq 1.8$ GPa the low-temperature value of f reaches almost 1.0. Given that in KFe_2As_2 bulk superconductivity is observed up to at least $P \simeq 6$ GPa [10], we conclude that for $P >$ 1.8 GPa bulk magnetism and bulk superconductivity coexist within the whole sample volume. Note that a similar type of bulk coexistence between the antiferromagnetic order and superconductivity was previously reported for various compounds belonging to the so-called 11 [29–35], 122 [36–51], 1144 [52–55], and 21311 [56] families of Fe-SCs.

The much weaker pressure-induced magnetism in $CsFe_2As_2$ and $RbFe_2As_2$ was probed via a direct comparison between the low- and the high-pressure data,

$$P_s^p(t) = P_s^{0.2\ \mathrm{GPa}}(t)e^{-\Delta\lambda(t)}. \quad (3)$$

Here, $P_s^{0.2\ \mathrm{GPa}}(t)$ is the time evolution of the muon-spin polarization measured at $P \simeq 0.2$ GPa (low pressure) and $\Delta\lambda$ is the additional exponential relaxation caused by pressure. The solid lines in Figs. 1(c)–(f) represent the result of the fit of Eq. (1) to the ZF-μSR $CsFe_2As_2$ and $RbFe_2As_2$ data with the sample part described by Eq. (3).

Figure 3 summarizes the results of our ZF-μSR study on a f-P and $\Delta\lambda$-P phase diagrams. For comparison we have also plotted the $T_c(P)$ curves as obtained in resistivity, magnetization, and transverse-field μSR experiments [8,11,20,57]. The gray stripes indicate the critical pressure regions: $P_c \simeq 1.75$, 1.4, and 1.1 GPa for KFe_2As_2, $CsFe_2As_2$, and $RbFe_2As_2$, respectively. In KFe_2As_2 the magnetic volume fraction increases rapidly from nearly zero to ~100% between 1.5 and 1.8 GPa, at least at the lowest temperature $T \simeq 0.27$ K [Fig. 3(d)]. In $CsFe_2As_2$ and $RbFe_2As_2$ [Figs. 3(e) and 3(f)] an additional exponential relaxation $\Delta\lambda$ goes to saturation for P exceeding ≃1.5 and ≃1.2 GPa, respectively. It is remarkable that in all three systems the magnetism develops *closely* to the P_c, i.e., to the pressure where the $T_c(P)$ curve acquires the positive slope.

It appears therefore that the disordered magnetism (which is static at least in the case for KFe_2As_2 [28]) supports (or even enhances) superconductivity in all three systems studied. This is unusual, as static magnetic order typically tends to compete with superconductivity. Note, however, that the magnetism we detect appears to be highly disordered and as such does not break translational symmetry on a sufficient length scale to cause the usual Fermi-surface reconstruction that is

detrimental to superconductivity. Indeed, no change is detected in the Fermi surface across P_c [7–11]. The cooperative nature of the interplay between magnetism and superconductivity is also reflected by the fact that the magnetism enhances significantly below T_c in the case of KFe_2As_2 [Figs. 2 and 3(a)] and develops just below T_c in the case of $CsFe_2As_2$ and $RbFe_2As_2$ [Figs. 3(b) and 3(d)].

This work was performed at the Swiss Muon Source (SμS), Paul Scherrer Institute (PSI, Switzerland). The authors are grateful to L. Taillefer for initiating the work and for helpful scientific discussions at the beginning of the project. A. Amato is acknowledged for help during the μSR experiments. R.K. acknowledges supporting discussions with J. Mesot.

[1] D. C. Johnston, Adv. Phys. **59**, 803 (2010).
[2] A. Chubukov, Annu. Rev. Condens. Matter Phys. **3**, 57 (2012).
[3] D. V. Evtushinsky, D. S. Inosov, V. B. Zabolotnyy, M. S. Viazovska, R. Khasanov, A. Amato, H.-H. Klauss, H. Luetkens, Ch. Niedermayer, G. L. Sun, V. Hinkov, C. T. Lin, A. Varykhalov, A. Koitzsch, M. Knupfer, B. Büchner, A. A. Kordyuk, and S. V. Borisenko, New J. Phys. **11**, 055069 (2009).
[4] P. J. Hirschfeld, M. M. Korshunov, and I. I. Mazin, Rep. Prog. Phys. **74**, 124508 (2011).
[5] S. Graser, T. A. Maier, P. J. Hirschfeld, and D. J. Scalapino, New J. Phys. **11**, 025016 (2009).
[6] R. M. Fernandes and A. J. Millis, Phys. Rev. Lett. **110**, 117004 (2013).
[7] F. F. Tafti, A. Juneau-Fecteau, M.-È. Delage, S. René d Cotret, J.-Ph. Reid, A. F. Wang, X.-G. Luo, X. H. Chen, N. Doiron-Leyraud, and L. Taillefer, Nat. Phys. **9**, 349 (2013).
[8] F. F. Tafti, J. P. Clancy, M. Lapointe-Major, C. Collignon, S. Faucher, J. A. Sears, A. Juneau-Fecteau, N. Doiron-Leyraud, A. F. Wang, X. G. Luo, X. H. Chen, S. Desgreniers, Y.-J. Kim, and L. Taillefer, Phys. Rev. B **89**, 134502 (2014).
[9] T. Terashima, K. Kihou, K. Sugii, N. Kikugawa, T. Matsumoto, S. Ishida, C.-H. Lee, A. Iyo, H. Eisaki, and S. Uji, Phys. Rev. B **89**, 134520 (2014).
[10] V. Taufour, N. Foroozani, M. A. Tanatar, J. Lim, U. Kaluarachchi, S. K. Kim, Y. Liu, T. A. Lograsso, V. G. Kogan, R. Prozorov, S. L. Budko, J. S. Schilling, and P. C. Canfield, Phys. Rev. B **89**, 220509(R) (2014).
[11] F. F. Tafti, A. Ouellet, A. Juneau-Fecteau, S. Faucher, M. Lapointe-Major, N. Doiron-Leyraud, A. F. Wang, X.-G. Luo, X. H. Chen, and L. Taillefer, Phys. Rev. B **91**, 054511 (2015).
[12] Z. Guguchia, A. Amato, J. Kang, H. Luetkens, P. K. Biswas, G. Prando, F. von Rohr, Z. Bukowski, A. Shengelaya, H. Keller, E. Morenzoni, R. Fernandes, and R. Khasanov, Nat. Commun. **6**, 8863 (2015).
[13] P. Wiecki, V. Taufour, D. Y. Chung, M. G. Kanatzidis, S. L. Bud'ko, P. C. Canfield, and Y. Furukawa, Phys. Rev. B **97**, 064509 (2018).
[14] V. Grinenko, W. Schottenhamel, A. U. B. Wolter, D. V. Efremov, S.-L. Drechsler, S. Aswartham, M. Kumar, S. Wurmehl, M. Roslova, I. V. Morozov, B. Holzapfel, B. Büchner, E. Ahrens, S. I. Troyanov, S. Köhler, E. Gati, S. Knöner, N. H. Hoang, M. Lang, F. Ricci, and G. Profeta, Phys. Rev. B **90**, 094511 (2014).
[15] B. Wang, K. Matsubayashi, J. Cheng, T. Terashima, K. Kihou, S. Ishida, C.-H. Lee, A. Iyo, H. Eisaki, and Y. Uwatoko, Phys. Rev. B **94**, 020502(R) (2016).
[16] S. Sachdev, Science **288**, 475 (2000).
[17] Z. Bukowski, S. Weyeneth, R. Puzniak, J. Karpinski, and B. Batlogg, Physica C **470**, S328 (2010).
[18] Z. Shermadini, J. Kanter, C. Baines, M. Bendele, Z. Bukowski, R. Khasanov, H.-H. Klauss, H. Luetkens, H. Maeter, G. Pascua, B. Batlogg, and A. Amato, Phys. Rev. B **82**, 144527 (2010).
[19] M. Rotter, M. Pangerl, M. Tegel, and D. Johrendt, Angew. Chem., Int. Ed. **47**, 7949 (2008).
[20] See Supplemental Material at http://link.aps.org/supplemental/10.1103/PhysRevB.102.140502 for a description of the sample characterization and for details of the ZF- and LF-μSR experiments on KFe_2As_2 and $CsFe_2As_2$ samples, which includes Refs. [58–62].
[21] R. Khasanov, Z. Guguchia, A. Maisuradze, D. Andreica, M. Elender, A. Raselli, Z. Shermadini, T. Goko, E. Morenzoni, and A. Amato, High Press. Res. **36**, 140 (2016).
[22] Z. Shermadini, R. Khasanov, M. Elender, G. Simutis, Z. Guguchia, K. V. Kamenev, and A. Amato, High Press. Res. **37**, 449 (2017).
[23] A. Suter and B. M. Wojek, Phys. Proc. **30**, 69 (2012).
[24] A. Yaouanc and P. Dalmas de Réotier, *Muon Spin Rotation, Relaxation and Resonance* (Oxford University Press, Oxford, U.K., 2011).
[25] R. E. Walstedt and L. R. Walker, Phys. Rev. B **9**, 4857 (1974).
[26] Z. L. Mahyari, A. Cannell, C. Gomez, S. Tezok, A. Zelati, E. V. L. de Mello, J. Q. Yan, D. G. Mandrus, and J. E. Sonier, Phys. Rev. B **89**, 020502(R) (2014).
[27] K. Ohishi (private communication).
[28] In the case of $CsFe_2As_2$ and $RbFe_2As_2$ it is difficult to draw conclusions from the decoupling LF experiments. The electronic relaxation of the pressure cell material reaches the value of $\simeq 0.3\mu s^{-1}$ at $T \simeq 0.25$ K [21], and it decouples at applied longitudinal field of $\sim$10 mT, i.e., in the same range of fields as expected for the decoupling of weak magnetism of $CsFe_2As_2$ and $RbFe_2As_2$.
[29] M. Bendele, A. Amato, K. Conder, M. Elender, H. Keller, H.-H. Klauss, H. Luetkens, E. Pomjakushina, A. Raselli, and R. Khasanov, Phys. Rev. Lett. **104**, 087003 (2010).
[30] R. Khasanov, M. Bendele, A. Amato, K. Conder, H. Keller, H.-H. Klauss, H. Luetkens, and E. Pomjakushina, Phys. Rev. Lett. **104**, 087004 (2010).
[31] M. Bendele, A. Ichsanow, Yu. Pashkevich, L. Keller, Th. Strässle, A. Gusev, E. Pomjakushina, K. Conder, R. Khasanov, and H. Keller, Phys. Rev. B **85**, 064517 (2012).
[32] K. Kothapalli, A. Böhmer, W. Jayasekara,, B. G. Ueland, P. Das, A. Sapkota, V. Taufour, Y. Xiao, E. Alp, S. L. Bud'ko, P. C. Canfield, A. Kreyssig, and A. I. Goldman, Nat Commun **7**, 12728 (2016).
[33] A. E. Böhmer, K. Kothapalli, W. T. Jayasekara, J. M. Wilde, B. Li, A. Sapkota, B. G. Ueland, P. Das, Y. Xiao, W. Bi, J. Zhao, E. E. Alp, S. L. Bud'ko, P. C. Canfield, A. I. Goldman, and A. Kreyssig, Phys. Rev. B **100**, 064515 (2019).

[34] S. Holenstein, U. Pachmayr, Z. Guguchia, S. Kamusella, R. Khasanov, A. Amato, C. Baines, H.-H. Klauss, E. Morenzoni, D. Johrendt, and H. Luetkens, Phys. Rev. B **93**, 140506(R) (2016).

[35] S. Holenstein, J. Stahl, Z. Shermadini, G. Simutis, V. Grinenko, D. A. Chareev, R. Khasanov, J.-C. Orain, A. Amato, H.-H. Klauss, E. Morenzoni, D. Johrendt, and H. Luetkens, Phys. Rev. Lett. **123**, 147001 (2019).

[36] A. I. Goldman, D. N. Argyriou, B. Ouladdiaf, T. Chatterji, A. Kreyssig, S. Nandi, N. Ni, S. L. Bud'ko, P. C. Canfield, and R. J. McQueeney, Phys. Rev. B **78**, 100506(R) (2008).

[37] S. Avci, O. Chmaissem, E. A. Goremychkin, S. Rosenkranz, J.-P. Castellan, D. Y. Chung, I. S. Todorov, J. A. Schlueter, H. Claus, M. G. Kanatzidis, A. Daoud-Aladine, D. Khalyavin, and R. Osborn, Phys. Rev. B **83**, 172503 (2011).

[38] M. G. Kim, D. K. Pratt, G. E. Rustan, W. Tian, J. L. Zarestky, A. Thaler, S. L. Bud'ko, P. C. Canfield, R. J. McQueeney, A. Kreyssig, and A. I. Goldman, Phys. Rev. B **83**, 054514 (2011).

[39] A. Kreyssig, M. G. Kim, S. Nandi, D. K. Pratt, W. Tian, J. L. Zarestky, N. Ni, A. Thaler, S. L. Bud'ko, P. C. Canfield, R. J. McQueeney, and A. I. Goldman, Phys. Rev. B **81**, 134512 (2010).

[40] P. Wang, Z. M. Stadnik, J. Zukrowski, A. Thaler, S. L. Bud'ko, and P. C. Canfield, Phys. Rev. B **84**, 024509 (2011).

[41] H. Luo, R. Zhang, M. Laver, Z. Yamani, M. Wang, X. Lu, M. Wang, Y. Chen, S. Li, S. Chang, J. W. Lynn, and P. Dai, Phys. Rev. Lett. **108**, 247002 (2012).

[42] S. Nandi, M. G. Kim, A. Kreyssig, R. M. Fernandes, D. K. Pratt, A. Thaler, N. Ni, S. L. Bud'ko, P. C. Canfield, J. Schmalian, R. J. McQueeney, and A. I. Goldman, Phys. Rev. Lett. **104**, 057006 (2010).

[43] P. Marsik, K. W. Kim, A. Dubroka, M. Rössle, V. K. Malik, L. Schulz, C. N. Wang, C. Niedermayer, A. J. Drew, M. Willis, T. Wolf, and C. Bernhard, Phys. Rev. Lett. **105**, 057001 (2010).

[44] A. D. Christianson, M. D. Lumsden, S. E. Nagler, G. J. MacDougall, M. A. McGuire, A. S. Sefat, R. Jin, B. C. Sales, and D. Mandrus, Phys. Rev. Lett. **103**, 087002 (2009).

[45] D. K. Pratt, M. G. Kim, A. Kreyssig, Y. B. Lee, G. S. Tucker, A. Thaler, W. Tian, J. L. Zarestky, S. L. Bud'ko, P. C. Canfield, B. N. Harmon, A. I. Goldman, and R. J. McQueeney, Phys. Rev. Lett. **106**, 257001 (2011).

[46] E. Wiesenmayer, H. Luetkens, G. Pascua, R. Khasanov, A. Amato, H. Potts, B. Banusch, H.-H. Klauss, and D. Johrendt, Phys. Rev. Lett. **107**, 237001 (2011).

[47] C. Bernhard, C. N. Wang, L. Nuccio, L. Schulz, O. Zaharko, J. Larsen, C. Aristizabal, M. Willis, A. J. Drew, G. D. Varma, T. Wolf, and Ch. Niedermayer, Phys. Rev. B **86**, 184509 (2012).

[48] Z. Li, R. Zhou, Y. Liu, D. L. Sun, J. Yang, C. T. Lin, and G.-q. Zheng, Phys. Rev. B **86**, 180501(R) (2012).

[49] P. Materne, S. Kamusella, R. Sarkar, T. Goltz, J. Spehling, H. Maeter, L. Harnagea, S. Wurmehl, B. Büchner, H. Luetkens, C. Timm, and H.-H. Klauss, Phys. Rev. B **92**, 134511 (2015).

[50] S. Kawasaki, T. Mabuchi, S. Maeda, T. Adachi, T. Mizukami, K. Kudo, M. Nohara, and G.-Q. Zheng, Phys. Rev. B **92**, 180508(R) (2015).

[51] E. Sheveleva, B. Xu, P. Marsik, F. Lyzwa, B. P. P. Mallett, K. Willa, C. Meingast, Th. Wolf, T. Shevtsova, Yu. G. Pashkevich, and C. Bernhard, Phys. Rev. B **101**, 224515 (2020).

[52] Q.-P. Ding, W. R. Meier, A. E. Böhmer, S. L. Bud'ko, P. C. Canfield, and Y. Furukawa, Phys. Rev. B **96**, 220510(R) (2017).

[53] S. L. Bud'ko, V. G. Kogan, R. Prozorov, W. R. Meier, M. Xu, and P. C. Canfield, Phys. Rev. B **98**, 144520 (2018).

[54] A. Kreyssig, J. M. Wilde, A. E. Böhmer, W. Tian, W. R. Meier, Bing Li, B. G. Ueland, Mingyu Xu, S. L. Bud'ko, P. C. Canfield, R. J. McQueeney, and A. I. Goldman, Phys. Rev. B **97**, 224521 (2018).

[55] R. Khasanov, G. Simutis, Y. G. Pashkevich, T. Shevtsova, W. R. Meier, M. Xu, S. L. Bud'ko, V. G. Kogan, and P. C. Canfield, Phys. Rev. B **102**, 094504 (2020).

[56] S. Holenstein, F. Hummel, Z. Guguchia, S. Kamusella, N. Barbero, H. Ogino, Z. Shermadini, R. Khasanov, A. Amato, T. Shiroka, H.-H. Klauss, E. Morenzoni, D. Johrendt, H. Luetkens, arXiv:1911.04319.

[57] Z. Shermadini, H. Luetkens, A. Maisuradze, R. Khasanov, Z. Bukowski, H. H. Klauss, and A. Amato, Phys. Rev. B **86**, 174516 (2012).

[58] R. Khasanov *et al.* (unpublished).

[59] R. Khasanov, H. Luetkens, A. Amato, H.-H. Klauss, Z.-A. Ren, J. Yang, W. Lu, and Z.-X. Zhao, Phys. Rev. B **78**, 092506 (2008).

[60] A. Schenck, *Muon Spin Rotation: Principles and Applications in Solid State Physics* (Adam Hilger, Bristol, 1986).

[61] R. Khasanov, K. Conder, E. Pomjakushina, A. Amato, C. Baines, Z. Bukowski, J. Karpinski, S. Katrych, H.-H. Klauss, H. Luetkens, A. Shengelaya, and N. D. Zhigadlo, Phys. Rev. B **78**, 220510(R) (2008).

[62] R. Khasanov, A. Maisuradze, H. Maeter, A. Kwadrin, H. Luetkens, A. Amato, W. Schnelle, H. Rosner, A. Leithe-Jasper, and H.-H. Klauss, Phys. Rev. Lett. **103**, 067010 (2009).